Osteoporos Int (2005) 16: S25–S35
DOI 10.1007/s00198-004-1701-7

ORIGINAL ARTICLE

Long-term prediction of three-dimensional bone architecture in simulations of pre-, peri- and post-menopausal microstructural bone remodeling

Ralph Müller

Received: 4 June 2004 / Accepted: 9 June 2004 / Published online: 31 August 2004

Abstract The mechanical behavior of trabecular bone depends on the internal bone structure. It is generally accepted now that the trabecular bone structure is a result of a load adaptive bone remodeling. The mathematical laws that relate bone remodeling to the local state of stress and strain, however, are still under investigation. The aim of this project was to investigate if changes in the trabecular architecture as observed with age-related bone loss and osteoporosis can be predicted from a computer model that simulates bone resorption after hormone depletion based on realistic models of trabecular microstructure using micro-computed tomography (μCT). A compact desktop μCT providing a nominal isotropic resolution of 14 μm was used to measure two groups of seven trabecular bone specimens from pre-menopausal and post-menopausal women respectively. A novel algorithm was developed to simulate age-related bone loss for the specimens in the first group. The algorithm, also referred to as simulated bone atrophy (SIBA), describes a truly three-dimensional approach and is based directly on cellular bone remodeling with an underlying realistic time frame. Bone resorption is controlled by osteoclastic penetration depth and bone formation is governed by the efficiency level of the osteoblasts. The simulation itself describes an iterative process with a cellular remodeling cycle of 197 days. Activation frequency is controllable and can be adjusted for the different phases of pre-, peri- and post-menopause. For our simulations, osteoblastic and osteoclastic activities were in balance until the onset of menopause, set to be at the age of 50 years. In that period, the structure remained almost constant. After the onset of menopause an imbalance in the cell activities was modeled resulting in a net bone loss. The doubling of the activation frequency in the peri-menopausal phase caused a pronounced loss. Using advanced animation tools and quantitative bone morphometry, the changes in bone architecture associated with the bone loss were monitored over an average observation time of 43 years until the age of 80 years. In that time, bone volume density decreased monotonously with the progression of the simulation for all specimens. Right after the onset of menopause, bone was lost fast, where with the progression of age losses slowed down. The structures at the end-point of the simulations were then compared qualitatively and quantitatively to the structures of the post-menopausal group with all morphometric indices being within a narrow margin of error. These results suggest the feasibility of transforming ''normal'' to ''osteopenic'' bone on a microstructural level yielding in realistic bone models similar in appearance as well as in structural behavior if compared to a post-menopausal group of women.

Keywords Age-related bone loss · Bone remodeling · Micro-computed tomography (μCT) · Osteoporosis · Trabecular bone architecture

R. Müller
Institute for Biomedical Engineering,
Swiss Federal Institute of Technology (ETH) and
University of Zürich, Moussonstrasse 18,
8044 Zürich, Switzerland
E-mail: rmueller@biomed.ee.ethz.ch
Tel.: +41-1-6324592
Fax: +41-1-6321214

Introduction

Osteoporosis occurs most frequently in post-menopausal women and the aged. It is defined as a systemic skeletal disease characterized by low bone mass and micro-architectural deterioration of bone tissue. Currently osteoporosis is considered an epidemic in the United States with approximately one-third of women over the age of 65 afflicted with the disease [1]. The reduced quality of osteoporotic bone greatly increases the risk of fractures [2,3]. As a result, health care costs related to osteoporotic fractures neared $14 billion in 1995 [4]. Although many older persons may lose bone, not all

develop fractures. The mechanical behavior of bone depends on the internal bone structure as well as the loads applied. It is also widely assumed that mechanical stresses and strains influence the remodeling process and subsequently the structure and strength of the bone. This adaptive response is generally referred to as Wolff's law after the German anatomist who first called attention to it. In 1892, Wolff [5] postulated that the trajectories of the trabecular bone align with the principal stress trajectories. Although the basic concepts of Wolff's law are generally accepted, the mathematical laws relating bone remodeling to the stress/strain relations are still under investigation.

Traditionally, animal experiments have been employed to investigate bone response from load alterations or during the progress of age-related bone loss. Since the time scale of the remodeling process is of the order of months or years, computational modeling offers a unique approach to study long term processes without the inconveniences of animal experimentation. Computer modeling is reliable, inexpensive and fast, and thus different optimization goals can be tried systematically until shape and architecture of bone can be reproduced. Mathematical formulations of Wolff's law for trabecular bone remodeling have been based on two general approaches. The first method is the development of empirical stress/morphology relationships that relate experimental measures of trabecular architecture to finite element estimates of stress distributions [6]. The second method is the development of iterative algorithms to predict load-driven bone adaptation based on the stress/strain state, again using finite element techniques to predict stress and strain distributions [7,8,9,10,11,12,13,14,15].

Since the work of Frost in the early 1960s, bone has been considered to remodel in discrete localized regions. All cells participating in the remodeling process have been termed the bone multicellular unit (BMU) and are thought to proceed through activation, resorption, and formation [16]. Remodeling has been proposed to function as a method of preventing the accumulation of fatigue damage and maintaining an adequate supply of relatively low mineral density bone to subserve mineral homeostasis. But what happens when the bone loses its ability for load-driven adaptation, when microdamage is no longer repaired, as seems to be the case for bone loss associated with age, medication or diseases? In these cases, the bone is left with its function to renew old bone, where each remodeling cycle seems to involve a net loss of bone mass, and as a consequence of this slightly negative balance between osteoclastic and osteoblastic activity, thinning of trabeculae and an increase in trabecular spacing take place. Therefore, bone gradually loses its strength over time.

The aim of this project was to investigate if changes in trabecular architecture as observed with age-related bone loss and osteoporosis can be predicted from a computer model that simulates bone resorption after hormone depletion over several decades based on realistic three-dimensional microstructural models of trabecular bone. Today, such models can be generated directly using either the destructive method of serial sectioning [17] or by employing non-destructive three-dimensional imaging techniques like micro-computed tomography (μCT) [18,19,20]. In this study, we used models of trabecular bone imaged with a compact desktop μCT system [21]. For the purpose of the study, two groups of seven specimens were defined for a pre-menopausal and a post-menopausal group of women. A novel algorithm was developed to simulate age-related bone loss for the specimens in the first group. The algorithm, also referred to as simulated bone atrophy (SIBA), describes an iterative, truly three-dimensional approach based on cellular bone remodeling and, for the first time, an underlying realistic time frame. The pre- and post-menopausal group as well as the set of simulations were analysed and compared using three-dimensional quantitative bone morphometry and newly developed animation techniques to visualize and monitor changes in trabecular bone architecture over several decades.

Materials and methods

Two groups of seven trabecular bone specimens were selected from a larger pool of data from the European Union BIOMED1 Concerted Action ''Assessment of Bone Quality in Osteoporosis'', where cylindrical bone biopsies from different anatomical locations were harvested post-mortem from 32 females and 38 males [22]. Donor age in the BIOMED1 study ranged from 23 to 92 years, with a mean age of 68 ± 16 years. The study included samples from the iliac crest (IC, transiliac), the femoral head (FH), the lumbar spine (L2 and L4) and the calcaneus (CA) for every subject [23]. The two subgroups included four trabecular bone cores from the iliac crest (IC) and three from the lumbar spine (L2) site each and were chosen to represent a pre-menopausal (36.7 ± 9.5 years) and a post-menopausal (77.4 ± 3.3 years) group of women, respectively. The criteria for the pre-menopausal group were an age of less than 50 years and a medical record showing no known bone disorders. For the post-menopausal group, only women in the 7th and 8th decade of their life were included as a consecutive sample. The goal was to have a cross-section of the BIOMED1 population rather than a selected group of individuals that could be considered normal or osteoporotic.

Three-dimensional microstructural imaging

To generate the three-dimensional models of microstructural bone, the selected biopsies were measured using a micro-tomographic imaging system (μCT 20; Scanco Medical, Bassersdorf, Switzerland), a compact fan-beam type of tomograph, also referred to as desktop μCT. The system was especially designed for the

non-destructive measurement and analysis of unprocessed surgical bone biopsies [21]. For each sample, a total of 286 micro-tomographic slices was acquired. Measurements were stored in three-dimensional image arrays. The total examination time per specimen was approximately 3 h for a voxel size of 14 μm.

A three-dimensional Gaussian filter with a limited, finite filter support was used to partly suppress the noise in the volumes. In the next step, the bone tissue was segmented from marrow and solution with the help of a thresholding procedure. All samples were binarized using the same parameters for the filter width (1.2), the filter support [2] and the threshold (10.2% of the maximal attenuation) [21]. For the subsequent simulation, a subvolume of the originally measured data was selected including only binarized trabecular plates and rods. This selected volume of interest (VOI) was located in the center of the specimen to eliminate preparation artifacts on the surface. The size of the VOI was always 3.6×3.6×3.6 mm (256×256×256 voxels).

Simulated bone atrophy and age-related bone loss

Thomsen et al. [24] developed a computer simulation model that could assist in predicting the long-term effect of changes in the remodeling process on bone mass, trabecular thickness, and perforations. They presented a stochastic model of the remodeling process in human vertebral trabecular bone, where the model is based on histomorphometric and structural data from human studies. The model describes the variation in bone mass, average trabecular thickness and number of perforations over an extended period of time. We wanted to take that approach one step further and introduce a model directly based on realistic three-dimensional trabecular bone structures. In order to include the three-dimensional bone architecture in the modeling, we introduced the concept of non-invasive bone biopsy [25], where the three-dimensional structure of trabecular bone was acquired non-invasively by a high-resolution quantitative CT system for peripheral measuring sites. Based on non-invasive bone biopsy, we developed a novel bone resorption algorithm to investigate the biomechanical consequences of age- and disease-related bone loss [26]. In that approach, bone loss was expressed as a decrease in bone density in combination with topological alterations of the bone structure. In order to be able to control the process of bone loss, an algorithm to simulate bone resorption and adaptive processes based on discrete volume data was developed. The algorithm, also referred to as simulated bone atrophy (SIBA), generated a set of microstructural models, all derived from the same original structure. Generally, the models varied in respect to both apparent density and the degree of structural anisotropy. The algorithm did not include a proposal for a new mathematical formulation of bone adaptation but more based on a phenomenological approach and observations made by other researchers of how bone structures change with age or loading [27,28]. Because the spatial resolution of the QCT measuring system (250 μm) and the mean trabecular width (80–150 μm) were of the same order, it was not yet possible to resolve the true shape of individual trabeculae. It was, however, possible to segment the trabeculae due to their large separation (400–1200 μm). Nonetheless, to implement a computer simulation of age-related bone loss directly based on osteoblastic and osteoclastic activity, which is the goal of this project, it seems to be necessary to have a resolution on the order of 20 μm or better as provided by the desktop micro-tomography system described earlier. To come up with a cell-based approach, the original SIBA algorithm had to be extended to allow an iterative approach directly associated with an underlying physical time frame and to reformulate the laws for bone resorption in the simulated bone atrophy.

The extended SIBA algorithm is based on the remodeling sequence first described by Frost [29], which consists of three phases: resorption, reversal, and formation. Thomsen et al. [24] used an iterative approach for their stochastic model and the time interval between iterations was 1 day. In our approach [30], one iteration would include all three steps, where bone resorption (osteoclastic activity) and bone formation (osteoblastic activity) would be modeled for each iteration. Nevertheless, the timeframe for the total remodeling cycle was chosen to equal 197 days to meet the average remodeling cycle time from the Thomsen study. Furthermore, the algorithm is based on the assumption that for normal bone osteoclastic and osteoblastic activity are in balance resulting in an almost stable bone mass and bone structure. After the onset of menopause, which was assumed to be at the age of 50 years, the balance would become negative, i.e. more bone is resorbed than formed, resulting in a net loss of bone mass. No further information was needed to run the models. The changes in architecture, we observed, were therefore only the result of the loss in bone mass over the years, which means that the architecture as it was present before menopause already predetermined the outcome in the simulated bone atrophy with a given, constant loss of bone. In the simulation, osteoclastic activity is modeled as an exponential function, i.e. the probability for bone being resorbed at a certain location in the bone matrix has a Gaussian profile. In practical terms, this means that the algorithm, applied to the digitized trabecular bone structure, is based on constrained Gauss filtration of binary data sets, i.e. only bone and non-bone will be differentiated. The effect of the Gaussian filter is mainly controlled by the filter width and the constrained filter support. Constrained, in this sense, means that the discrete convolution of the Gaussian and the binary data set is computed only for a limited, finite filter support. In our case, we used a filter support of 2, which means that a newly computed value only depended on the sum of the weighted values of the point's direct neighborhood (5×5×5). This also means that an osteoclast can penetrate into the bone only two voxels per cycle, which

corresponds to a perforation depth ranging between 28 and 48 μm depending on the neighborhood configuration. Since the original structures were based on binary data, every data point in the volume has either a value of one or zero prior to the filtration. The constrained Gauss filtration will result in a gray-scale data set with values between zero and one. The more data points are "set" in the weighted neighborhood the higher the resulting gray-scale values and vice versa. Therefore, the application of the Gaussian filter introduces a small gradient on the surface of the structure, whereas values in the center of the structure, totally surrounded by mineralized bone, will be unchanged. The total amount of bone mass in a local neighborhood (sum of weighted voxels) is the same before and after the filtration but the three-dimensional distribution of the mass has changed according to the local topology. In our simulation, the four phases in the remodeling cycle are fully synchronized for all cell activities in the structure, which means that in a first step bone is resorbed only and then in a second step bone is formed only. There is no temporal overlay of the osteoclastic and osteoblastic activity, which in reality is not the case and has therefore to be taken as a current limitation of the algorithm. Additionally, the amount of surface area involved in a remodeling cycle was not controlled, so that in the simulation the whole surface was affected by either osteoclastic or osteoblastic cell activity, which again in reality is most probably not the case. The amount of bone that is removed or added in one iteration step is controlled by setting a global threshold for the filtered data, which must be between 0 and 1. In our simulation, we found that a threshold of 0.5 (all voxels with a gray-scale value higher or equal to 0.5 are included) would allow maintenance of the total amount of mass. This was defined as the 100% efficiency level for the osteoblastic activity, which means that the osteoblasts were able to form as much bone as has been resorbed by the osteoclasts. A threshold of 1.0 on the other hand resulted in the removal of all elements with at least one zero voxel in their local 5×5×5 neighborhood, which would correspond to a 0% efficiency level. The relation between the threshold and the efficiency level can be expressed as a second order polynomial, which means that initially the efficiency is high and is dropping down quickly with increasing threshold.

Whereas the original implementation distinguished only between pre- and post-menopause [30], where changes were assumed to happen only after the onset of menopause, the current implementation includes three distinctively different stages, namely the pre-, peri- and post-menopause. Pre-menopause is the period of time after bone growth ceases and before menopause begins. Although bone loss in this stage is minimal, it is important to model the structural changes prior menopause. Without its inclusion, the changes that occur will be underestimated. The peri-menopausal stage is a period of about 5 years after the onset of menopause where the bone may actually undergo the most changes [31]. Experimental values from the literature were used to determine the values for osteoclastic perforation depth, the osteoblastic efficiency level and activation frequency. Activation frequency (AF) is defined as the rate at which bone multicellular units (BMU) are formed. Together with the individual cellular function rates at the BMU, it determines the percentage of bone turnover [32]. AF was not part of the original algorithm, where the length of one iteration was simply defined by the length of the remodeling cycle (197 days). In the present simulation, the length of one iteration was defined as 1/AF under the assumption that each BMU is activated in that time. Normal activation frequency was assumed at 1/1096 days [24], which corresponded to an iteration length of approximately 3 years. In peri-menopause, activation frequency was seen to double [33], which resulted in a cycle time of 1.5 years in our simulation. In order to establish a more realistic time frame and estimation for the values of the simulation parameters after the onset of menopause, the experimental post-menopausal group was used as a control group. The strategy was to adapt the osteoclastic efficiency level in a way to match the volumetric densities of simulation and experimental group at the end-point of the simulation. It is clear that such an approach can only be one of many scenarios of what could have happened to these pre-menopausal bone specimens with time. Important for us was to see whether the outcome of the simulation would result in reasonable and realistic structures if compared to the post-menopausal experimental group. The validation of the algorithm was therefore based on both a qualitative (visualization) and quantitative (morphometry) comparison between those two groups. For the three-dimensional visualization, an extended marching cubes algorithm was used [25]. The algorithm, which is based on a divide-and-conquer approach, triangulates the surface of any given voxel array in a fast and secure way. It not only allows perfect triangulation, but also smooths the surface effectively.

Direct quantitative bone morphometry

In addition to the visual assessment of structural changes with age, morphometric and architectural indices can be determined from the micro-tomographic examinations. In the past, structural properties of trabecular bone have been investigated by examination of two-dimensional sections of cancellous bone biopsies. Three-dimensional morphometric parameters are then derived from two-dimensional images using stereological methods [34,35]. While parameters like bone volume density (BV/TV) and surface density (BS/TV) can directly be obtained from two-dimensional images, a range of important parameters such as trabecular thickness (Tb.Th), trabecular separation (Tb.Sp), and trabecular number (Tb.N) are to be derived indirectly assuming a fixed structural model, typically an ideal plate or rod model is used. Such assumptions are, however, critical due to the well-known fact that trabecular bone con-

tinuously changes its structure type as a result of remodeling. A deviation from the assumed model will lead to an unpredictable error of the indirectly derived parameters. This is particularly true in this study, where we actually would like to follow the changes in bone structure in the course of age-related bone loss. In such a case, a predefined model assumption could easily over- or underestimate the effects of the bone atrophy depending on the assessed index. For these reasons and in order to take full advantage of the volumetric measuring technique, new methods that make direct use of the three-dimensional information are required. To meet this demand several new methods by means of three-dimensional image processing have recently been presented, allowing direct quantification of the actual architecture of trabecular bone. In this study, we used metric and also non-metric parameters entirely based on direct three-dimensional calculations. The definitions and methods used for the calculation of the model independent parameters have recently been developed and introduced for the microstructural evaluation of the BIOMED1 study [36].

In the presented approach, the volume of the trabeculae (BV) was calculated using tetrahedrons corresponding to the enclosed volume of the triangulated surface used for the surface area calculation. From this measure the relative bone volume (BV/TV) can be calculated. The total volume (TV) is the volume of the whole examined sample. The bone surface area (BS) was calculated using surface triangulation of the binary data [25]. The specific bone surface or bone surface-volume ratio is given by BS/BV. In conventional stereology, these primary parameters are then be used to derive other indices such as the trabecular thickness (Tb.Th), the trabecular separation (Tb.Sp) or the trabecular number (Tb.N) based on the underlying model assumption. An even more indirect way to calculate these metric parameters is to derive the involved surface area indirectly using methods such as mean intercept length or two-dimensional perimeter estimation. Such methods were developed for the two-dimensional analysis of trabecular bone, but are nevertheless used for the analysis of three-dimensional images [37]. A recent study showed that such indirectly derived primary quantities could vary as much as 52%, depending on which method is used [38]. A more direct approach to assess metric parameters from three-dimensional images is based on measuring actual distances in the three-dimensional space. Such techniques do not rely on an assumed model type and are therefore not biased by eventual deviations of the actual structures from this model. In such a way, mean trabecular thickness (Tb.Th) can be calculated directly and without an underlying model assumption by determining a local thickness at each voxel representing bone [39]. The same method can be used to calculate the mean trabecular separation (Tb.Sp) by applying the thickness calculation to the non-bone parts of the three-dimensional image. The separation is thus the thickness of the marrow cavities. Trabecular number (Tb.N) is defined for the plate model as the number of plates per unit length. An alternative geometrical interpretation can be formulated as the inverse distance between the midsection of the plates. For a general structure, it would be possible to assess the mean distance between the mid axes of the structure and use the inverse of this measure to calculate the mean number of elements per unit length. The mid-axes of the structure can be extracted from a binary three-dimensional image using different techniques [40]. In this implementation, three-dimensional distance transformation to extract the geometrical mid points of the structure was used [39]. To get a measure for mean distance between the points the direct thickness method similar to the Tb.Sp calculation was applied, i.e. the separation between the mid-axes was assessed. In addition to the computation of the direct metrical parameters, other non-metric parameters can be calculated to describe the three-dimensional nature of the bone structure. An estimation of the plate-rod characteristic of the structure can be obtained from the structure model index (SMI) [41]. SMI is calculated by a differential analysis of a triangulated surface of a structure. For an ideal plate and rod structure the SMI value is 0 and 3, respectively. For a structure with both plates and rods of equal thickness the value will be between 0 and 3, depending on the volume ratio between rods and plates. Another parameter often used as an architectural index is the geometrical anisotropy of a structure, which is typically determined using mean intercept length (MIL) measurements [42]. MIL denotes the average distance between bone/marrow interfaces and is measured by tracing test lines in different directions in the examined VOI. From this measurement, an MIL tensor can be calculated by fitting the MIL values to an ellipsoid. The eigenvalues of this tensor can then be used to define the degree of anisotropy (DA), which denotes the maximum to minimum MIL ratio.

Results

Bone atrophy simulation

First, a time-zero iteration with no associated time and bone loss was used to convert the measured bone specimen to a computer model. A sigma value of 0.5, a filter support of 2, and a 100% efficiency level were chosen. For each phase of the simulation, a set of parameters had to be determined and implemented. Individual differences between the specimens were not accounted for. All parameters were chosen to be homogenous for each of the three phases of pre-, peri- and post-menopause. For the pre-menopausal phase, an osteoclastic penetration depth of approximately 30 μm (sigma = 1.1, support = 2), an osteoclastic efficiency level of 99.7% (resulting in a decrease in volume density of 0.34% per year) and an AF of 1/1096 days were chosen. The number of iterations to reach the age of 50 years, the

assumed onset of menopause, varied between zero and nine depending on the individual age of the donor bone. The average bone loss that occurred was −5.6% over an average of 13.4 years of pre-menopause, which was consistent with the values found in the literature for that time period [43]. In peri-menopause the osteoclastic penetration depth was increased by 40% [24,44] changing the sigma from 1.1 to 1.5, the osteoclastic efficiency level was reduced to 95% and AF was doubled to 1/548 days [33] resulting in a total of four iterations needed to simulate 6 years of peri-menopause. Finally, in post-menopause, osteoclastic penetration depth and AF were set to the values for the pre-menopausal phase with a sigma of 1.1 and an AF of 1/1096 days, respectively. Post-menopause was simulated with a total of eight iterations concluding at the age of 80 years.

Simulated bone atrophy was applied to all seven pre-menopausal specimens resulting in 12–21 models of atrophied bone per specimen starting at the individual age of the donor bone until a simulated age of 80 years was reached. The average computer time needed for a full length simulation varied between 180 and 220 min per specimen using a personal workstation DEC 3000-M300LX (Digital Equipment Cooperation, Maynard, USA). After the simulations, three-dimensional visualizations as well as structural parameters using direct three-dimensional techniques were computed for the total of 129 microstructural bone models including pre-menopausal (7), post-menopausal (7), and all the simulations (115). In total, this accounted for a few weeks of computer time with an approximated 250 minutes of calculation time per model.

Qualitative and quantitative validation

In a first attempt to validate the algorithm, we simply compared the three-dimensional structures at the end-points of the simulations with the structures of the post-menopausal group on a visual basis. From that, we can conclude that the algorithm does in fact produce realistic structures comparable to the old-aged group. Figures 1 and 2 show examples for the iliac crest and the lumbar spine respectively. In the illustrations, the baseline structure of a pre-menopausal woman and the corresponding simulation are compared to the structure of a post-menopausal woman for both measurement sites. The distinct transformation of the trabecular bone architecture from a ''plate-like'' to a more ''rod-like'' structure in the course of age-related bone loss can easily be noticed. The advantage of simulated bone atrophy is that it generates not only static images at the end-point of the simulation but rather allows to follow the changes with age step by step as illustrated in Fig. 3, where we concentrated on a smaller detailed view of the structural changes from a simulation of an iliac crest bone sample. For a young and healthy subject as illustrated in the top-left corner of the figure we typically find a plate-like structure with smaller rods connecting the plates for both the iliac crest and the lumbar spine. With increasing age the plate-like structure is partly resolved into a rod-like structure. The rods forming the trabecular network are more and more thinned until they are eventually perforated. After they are disconnected they disappear quickly, leaving the structure more widely spaced and less well connected.

These changes were also reflected in the structural properties assessed by quantitative bone morphometry. The relative bone volume decreased monotonously with the progression of the simulation for all seven specimens (Fig. 4). Right after the onset of menopause, bone was lost fast, where with the progression of age the losses slowed down. When we looked at the relative changes over the course of the simulation, the different specimens lost different amounts of bone with $\Delta BV/TV$ ranging from 21% to 68% (Fig. 5). This is an interesting fact, since the efficiency level for bone formation controlling the net bone loss per iteration was set as identical for all specimens, and those specimens that lost bone ''fast'' were not associated with an especially high or low bone density.

This left architecture was the only independent factor in the simulation influencing the rate of bone loss, which means that the architecture itself determined whether an individual lost bone ''fast'' or ''slow'' in our simulation with a constant efficiency level and a constant

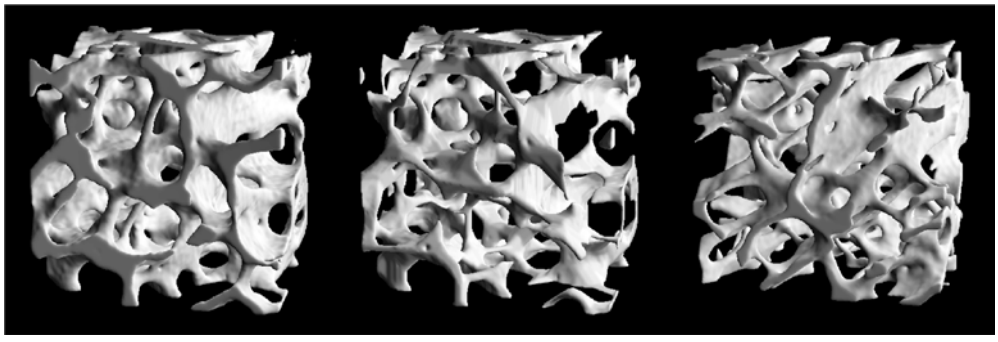

Fig. 1 Three-dimensional trabecular bone architecture of iliac crest bone biopsies of a 32-year-old (*left*), the corresponding ''80-year-old'' simulation (*middle*) and an 83-year-old (*right*) woman, respectively. Both the simulation and the structure from the age-matched group show a relative bone volume of 13% whereas the bone volume at the pre-menopausal baseline was measured at 21%

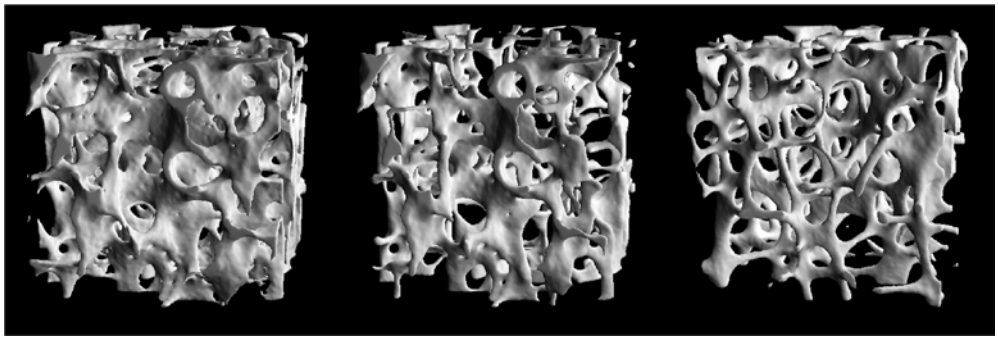

Fig. 2 Three-dimensional trabecular bone architecture of lumbar spine (L2) bone biopsies of a 50-year-old (*left*), the corresponding "80-year-old" simulation (*middle*) and an 80-year-old (*right*) woman, respectively. Both the simulation and the structure from the age-matched group show a relative bone volume of 7%, whereas the bone volume at the pre-menopausal baseline was measured at 11%

remodeling cycle time. When we looked at specific bone surface (Fig. 6), we noticed that BS/BV was increasing during the simulation but the effects were not as pronounced as for bone volume density. Nevertheless, the specific surface density at the age of 50 (start of menopause) predicted the total relative changes in bone volume density over 30 years with an r^2 of 0.96, which means that 96% of the changes in bone density over time could be predicted by the initial BS/BV measure (Fig. 7).

Mean trabecular thickness was not much affected by the simulation (approximately $\pm 10\%$), except for one specimen where we saw an decrease of about 20%, again showing the ability of the simulation to pick up individual differences in architecture. Trabecular separation showed similar although inverted trends as the primary parameter of bone volume with changes ranging from $+9\%$ up to $+19\%$. Tb.N on the other side was affected heavily by the procedure with changes from -17% to -55%, indicating that the simulated bone loss left the structure with fewer trabeculae. Structure model index supported the theory that trabecular bone is transformed from plate-like to rod-like in the progress of age-related bone loss with an initial mean value of 1.1 (0.5–2.1), indicating more plate-like structures (the value for a perfect plate model is 0) and a mean value of 1.8 (1.1–2.7) after the simulation indicating a transition to more rod-like structures (the value for a perfect rod model is 3). The most dramatic changes in SMI were found in the iliac crest specimens with an increase of over 150%. The

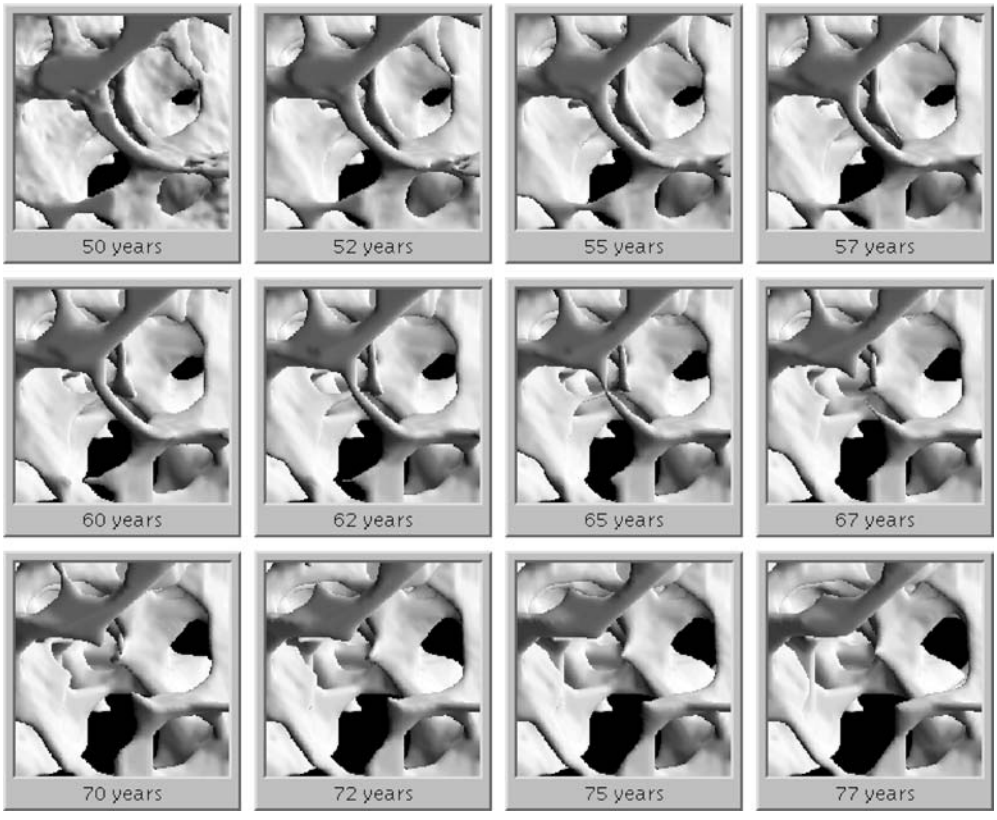

Fig. 3 Detail from the simulation of an iliac crest bone biopsy of a 47-year-old woman. The simulation illustrates the changes in bone architecture over time, where with increasing age the plate-like structure is partly resolved and with that transformed into a more rod-like structure. In this process, the rods forming the network are more and more thinned until they are eventually perforated. After a perforation takes place the remaining rod disappears quickly, leaving the structure more widely spaced and less well connected

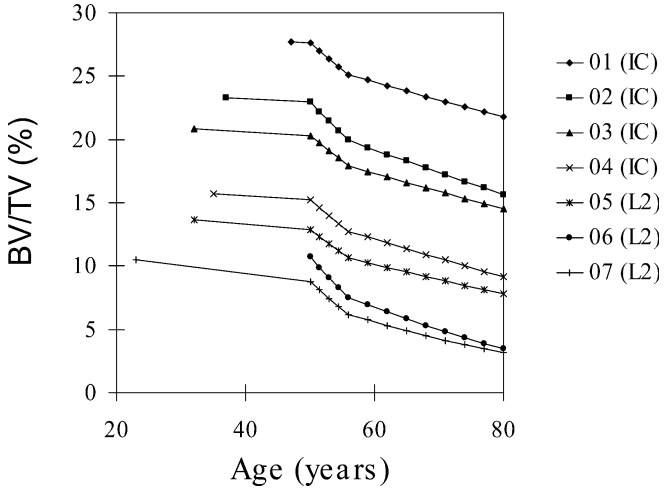

Fig. 4 BV/TV in the course of age-related bone loss as determined by simulated bone atrophy. The simulation started at the individual ages of each donor. The onset of menopause was assumed to be at the age of 50 years

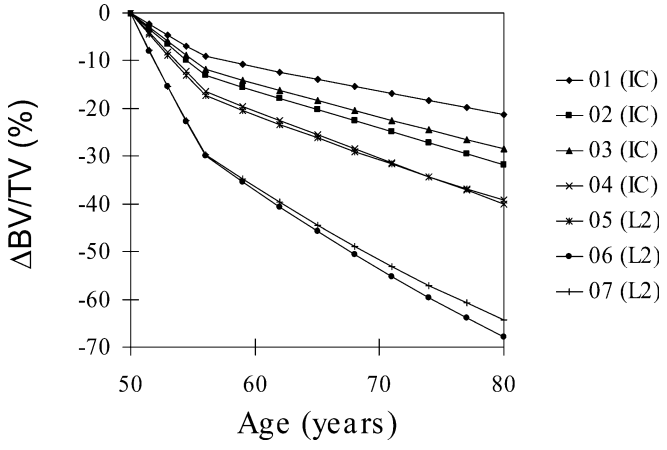

Fig. 5 Relative changes in BV/TV with respect to the simulated age starting at menopause

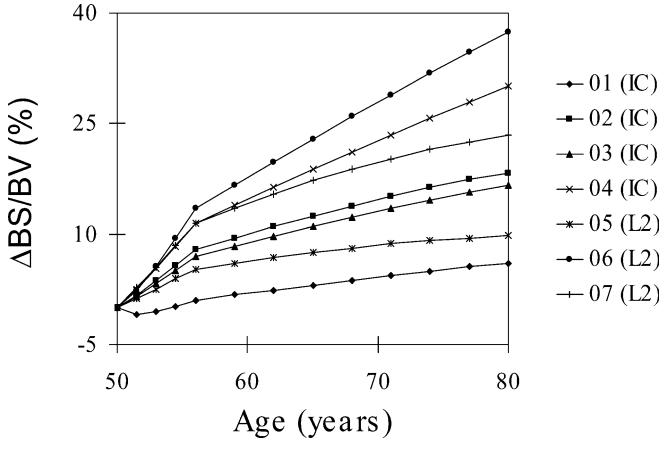

Fig. 6 Relative changes in BS/BV with respect to the simulated age starting at menopause

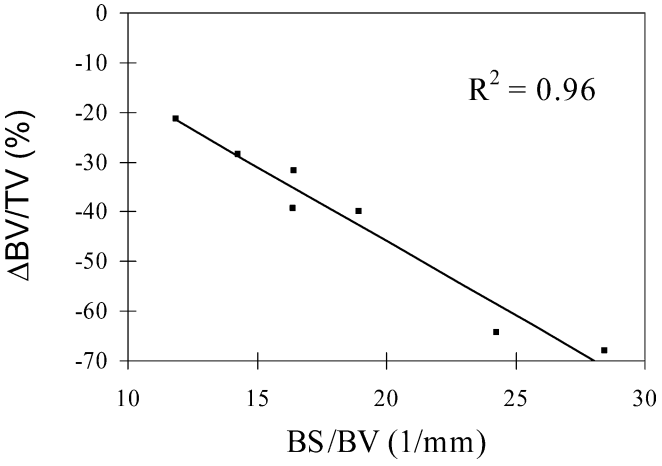

Fig. 7 BS/BV measured at menopause is highly correlated to the total amount of relative bone loss occurring over 3 decades

smallest changes were seen in the lumbar spine with an increase of SMI from 1.8 to 2.4 (+27%).

The results from the quantitative morphometry for the end-points of the simulation were then compared to the values of the post-menopausal group directly analysed after micro-tomographic imaging (Table 1). Since we used BV/TV to calculate the efficiency level, the two values for the simulation and the post-menopausal group had to be in full accordance and showed both an average decrease of 38% compared to the pre-menopausal baseline measurements. BS/BV, as the other primary parameter, only increased 12% for the post-menopausal group and 19% for the simulation group, respectively. Tb.N decreased 32% for the post-menopausal group and 37% for the simulation group respectively. Tb.Sp showed again similar results for the post-menopausal and the simulation group, with increases of 25% and 23% respectively, whereas Tb.Th showed a slight decrease of 11% for the post-menopausal group and a 4% increase for the simulation. If we look at the non-metric parameters, we find very similar results for the SMI with an increase of 72% and 77% respectively. DA, on the other hand, changed only moderately for the post-menopausal group with an increase of 7% whereas in the simulation the degree of anisotropy changed by 9%.

Discussion

The aim of this project was to develop an algorithm which allows simulation of the response of the trabecular bone in age-related bone loss and to determine the biomechanical consequences of such a response based on realistic three-dimensional models of the trabecular microstructure. Two groups of seven trabecular bone specimens were measured micro-tomographically, including specimens from pre-menopausal and post-menopausal women, respectively. In order to control bone loss over time, a novel algorithm to simulate bone

Table 1 Mean (SD) of assessed morphometric parameters

Parameters	Pre (exp.)	Peri	Peri post	Post	Post (exp.)
Age (years)	36.6 (9.3)	50	56	77	77.4 (3.3)
BV/TV (%)	17.9 (6.7)	17.3 (7.0)	14.6 (7.0)	11.0 (6.9)	11.0 (4.4)
BS/BV (1/mm)	19.1 (5.4)	18.6 (5.6)	20.2 (6.9)	22.8 (8.8)	21.4 (3.5)
Tb.N (1/mm)	1.6 (0.4)	1.5 (0.3)	1.3 (0.4)	1.0 (0.4)	1.1 (0.3)
Tb.Th (mm)	0.14 (0.03)	0.16 (0.05)	0.15 (0.05)	0.15 (0.05)	0.13 (0.02)
Tb.Sp (mm)	0.61 (0.10)	0.66 (0.07)	0.69 (0.08)	0.75 (0.10)	0.76 (0.10)
DA	1.2 (0.1)	1.3 (0.1)	1.3 (0.1)	1.4 (0.2)	1.3 (0.1)
SMI	1.0 (0.6)	1.1 (0.7)	1.4 (0.7)	1.8 (0.7)	1.7 (0.6)

resorption and adaptive processes was developed. Although the simulations were computationally very intensive, minimal user interaction was needed to build and analyze the models. All individual steps were fully automated. The algorithm, also referred to as simulated bone atrophy (SIBA), generated a set of microstructural models, iteratively derived from the original three-dimensional structure. Simulated bone atrophy was used to ''age-match'' the first and the second group incorporating an underlying realistic timeframe for the simulation. Using quantitative bone morphometry and three-dimensional animation tools, the changes in bone density and bone architecture could be monitored over an average observation time of 43 years until the age of 80 years. The structures at the simulated age of 77 years were then compared qualitatively and quantitatively to the structure of the post-menopausal group with an average age of 77.4 years. Good correspondence was found between the two groups. No significant changes could be detected between parameters from the simulation and the experimental group. Differences on the order of 10–20% can easily be accounted for given the huge biological variations of up to 50% in the different structural properties of trabecular bone as seen in the analysis of the BIOMED1 study [36].

Although there are several limitations to this study, we believe that we were able to demonstrate that it is possible to simulate, at least certain aspects, of age-related bone loss using the proposed mechanism. The implemented approach in combination with microstructural trabecular bone models allowed a successful transformation of ''young-and-normal'' to ''old-and-osteopenic'' bone on a microstructural level. Another advantage of the proposed model was that an identical remodeling law and time step was applied to both iliac and lumbar trabecular bone, which raises the question whether there is a universal law for all types of bone with respect to the effects on the cellular level. One of the limitations of simulated bone atrophy is that at the moment no experimental data is available to backup the proposed cellular mechanisms and that no mechanical feedback loop is included in the algorithm. This is especially important for simulation of bone modeling related to osteogenesis or fracture healing in healthy subjects with the ability to react to such changes in the overall loading patterns. For this reason, one of the future goals must be a combination of load and hormone driven modeling and remodeling on a microstructural level. Nevertheless, it might well be that to describe the effects purely associated with age-related bone loss in a hormone deficiency model, where bone seems to have at least partly lost its ability to adapt to alterations in its mechanical environment, load-driven modeling and remodeling might no longer have significant importance.

To our knowledge, this is the first time that age-related bone loss has been described and simulated directly based on three-dimensional measurements of trabecular bone with the incorporation of a realistic time frame. Although validation will be very difficult, it will be of crucial importance for further application of simulated bone atrophy. The only way to really validate any remodeling theory would be the incorporation of in vivo follow-up measurements providing not only important experimental data on the time-scale and structural properties of atrophied bone but also allowing validation of each remodeling step in the simulation. Kinney et al. [20] developed a CT-scanning method demonstrating sequential changes in bone structure at a resolution of a few microns. However, this resolution is only possible in animal experiments, due to dose considerations. Since we are interested in the prediction of the individual fracture risk of patients, the final aim must be the non-invasive assessment of the bone architecture in human subjects in vivo. In order to assess the structural changes in the progress of rapid bone loss, Müller et al. [45] introduced a method to assess and analyze cancellous bone based upon three-dimensional peripheral computed tomography in vivo. In their study, structural parameters could be reproduced in vivo with a coefficient of variation of less than 0.4% demonstrating the potential of high-resolution tomography to detect structural changes in trabecular bone during age-related bone loss or therapeutic and diagnostic trials. The nominal resolution provided by the system was 170 μm, which would not be sufficient for validation purposes. Today, there are new in vivo systems coming into the clinical market [46] providing even higher resolutions down on the order of 90 μm. Whether this resolution will be high enough allowing both simulations of bone adaptation with the possibility to non-invasively follow bone remodeling and adaptation in vivo will have to be investigated in future studies.

One other future goal of the project will be to investigate the consequences of bone atrophy on the mechanical behavior of the trabecular bone over time. Generally, the influence of the microstructural

adaptation on the biomechanical competence of the bone can be expressed as a function of its anisotropic bone properties on the continuum level. It has been shown that the mechanical properties of trabecular bone can be predicted using microstructural large-scale finite element analyses (FEA) [47,48,49]. The application of such simulations in combination with FEA of non-destructively assessed trabecular bone structures will help to understand the influence of age-related bone loss on the mechanical behavior of trabecular bone and will also be used to validate similar findings from follow-up patient measurements in vivo.

Acknowledgements The author gratefully acknowledges support from the Swiss National Science Foundation (no. 823A-043040). The author would also like to thank Jennifer Barragan for her help with the coding of the simulated bone atrophy algorithm.

References

1. Melton LJ, 3rd, Chrischilles EA, Cooper C, Lane AW, Riggs BL (1992) Perspective. How many women have osteoporosis? J Bone Miner Res 7:1005–1010
2. Kleerekoper M, Villanueva AR, Stanciu J, Rao DS, Parfitt AM (1985) The role of three-dimensional trabecular microstructure in the pathogenesis of vertebral compression fractures. Calcif Tissue Int 37:594–597
3. Kanis JA (1994) Osteoporosis and its consequences Osteoporosis. Blackwell Science, Oxford, pp 1–21
4. Ray NF, Chan JK, Thamer M, Melton LJ, 3rd (1997) Medical expenditures for the treatment of osteoporotic fractures in the United States in 1995: report from the National Osteoporosis Foundation. J Bone Miner Res 12:24–35
5. Wolff J (1892) Das Gesetz der Transformation der Knochen (The law of bone remodelling). Springer-Verlag, Berlin, Germany
6. Cheal EJ, Snyder BD, Nunamaker DM, Hayes WC (1987) Trabecular bone remodeling around smooth and porous implants in an equine patellar model. J Biomech 20:1121–1134
7. Hart RT, Davy DT, Heiple KG (1984) Mathematical modeling and numerical solutions for functionally dependent bone remodeling. Calcif Tissue Int 36:S104–109
8. Fyhrie DP, Carter DR (1986) A unifying principle relating stress to trabecular bone morphology. J Orthop Res 4:304–317
9. Carter DR (1987) Mechanical loading history and skeletal biology. J Biomech 20:1095–1109
10. Carter DR, Orr TE, Fyhrie DP (1989) Relationships between loading history and femoral cancellous bone architecture. J Biomech 22:231–244
11. Huiskes R, Weinans H, Grootenboer HJ, Dalstra M, Fudala B, Slooff TJ (1987) Adaptive bone-remodeling theory applied to prosthetic-design analysis. J Biomech 20:1135–1150
12. Cowin SC, Moss-Salentijn L, Moss ML (1991) Candidates for the mechanosensory system in bone. J Biomech Eng 113:191–197
13. Weinans H, Huiskes R, Grootenboer HJ (1992) The behavior of adaptive bone-remodeling simulation models. J Biomech 25:1425–1441
14. Huiskes R, Ruimerman R, van Lenthe GH, Janssen JD (2000) Effects of mechanical forces on maintenance and adaptation of form in trabecular bone. Nature 405:704–706
15. Ruimerman R, Van Rietbergen B, Hilbers P, Huiskes R (2003) A 3-dimensional computer model to simulate trabecular bone metabolism. Biorheology 40:315–320
16. Frost HM (1964) The laws of bone structure. Charles C. Thomas, Springfield
17. Odgaard A, Andersen K, Melsen F, Gundersen HJ (1990) A direct method for fast three-dimensional serial reconstruction. J Microsc 159:335–342
18. Feldkamp LA, Goldstein SA, Parfitt AM, Jesion G, Kleerekoper M (1989) The direct examination of three-dimensional bone architecture in vitro by computed tomography. J Bone Miner Res 4:3–11
19. Bonse U, Busch F, Gunnewig O, Beckmann F, Pahl R, Delling G, Hahn M, Graeff W (1994) 3D computed X-ray tomography of human cancellous bone at 8 microns spatial and 10(-4) energy resolution. Bone Miner 25:25–38
20. Kinney JH, Lane NE, Haupt DL (1995) In vivo, three-dimensional microscopy of trabecular bone. J Bone Miner Res 10:264–270
21. Rüegsegger P, Koller B, Müller R (1996) A microtomographic system for the nondestructive evaluation of bone architecture. Calcif Tissue Int 58:24–29
22. Dequeker J (1994) Assessment of quality of bone in osteoporosis—BIOMED I: fundamental study of relevant bone. Clin Rheumatol 13:7–12
23. Müller R, Rüegsegger P (1997) Micro-tomographic imaging for the nondestructive evaluation of trabecular bone architecture. Stud Health Technol Inform 40:61–79
24. Thomsen JS, Mosekilde L, Boyce RW, Mosekilde E (1994) Stochastic simulation of vertebral trabecular bone remodeling. Bone 15:655–66
25. Müller R, Hildebrand T, Rüegsegger P (1994) Non-invasive bone biopsy: a new method to analyse and display the three-dimensional structure of trabecular bone. Phys Med Biol 39:145–164
26. Müller R, Rüegsegger P (1996) Analysis of mechanical properties of cancellous bone under conditions of simulated bone atrophy. J Biomech 29:1053–1060
27. Mosekilde L (1988) Age-related changes in vertebral trabecular bone architecture—assessed by a new method. Bone 9:247–250
28. Parfitt AM (1992) Implications of architecture for the pathogenesis and prevention of vertebral fracture. Bone 13:S41–47
29. Frost HM 1969 Tetracycline-based histological analysis of bone remodeling. Calcif Tissue Res 3:211–237
30. Müller R, Hayes WC (1997) Biomechanical competence of microstructural bone in the progress of adaptive bone remodeling. In: Bonse U (ed) Developments in X-ray tomography, vol. 3149. San Diego, California, pp 69–81
31. Young R, May H, Murphy S, Grey C, Compston JE (1996) Rates of bone loss in peri- and postmenopausal women: a 4-year, prospective, population-based study. Clin Sci (Lond) 91:307–312
32. Eriksen EF, Langdahl B (1995) Bone remodeling and its consequences for bone structure. In: Odgaard A, Weinans H (eds) Bone structure and remodeling, recent advances in human biology, vol. 2. World Scientific, Singapore, pp 25–36
33. Brockstedt H, Kassem M, Eriksen EF, Mosekilde L, Melsen F (1993) Age- and sex-related changes in iliac cortical bone mass and remodeling. Bone 14:681–691
34. Schenk RK, Olah AJ (1980) Histomorphometrie. In: Kuhlencordt R, Bartelheimer H (eds) Hanbuch der inneren Medizin VI/a!, Knochen, Gelenke, Muskeln. Springer-Verlag, Berlin, pp 437–494
35. Parfitt AM, Drezner MK, Glorieux FH, Kanis JA, Malluche H, Meunier PJ, Ott SM, Recker RR (1987) Bone histomorphometry: standardization of nomenclature, symbols, and units. Report of the ASBMR Histomorphometry Nomenclature Committee. J Bone Miner Res 2:595–610
36. Hildebrand T, Laib A, Müller R, Dequeker J, Rüegsegger P (1999) Direct three-dimensional morphometric analysis of human cancellous bone: microstructural data from spine, femur, iliac crest, and calcaneus. J Bone Miner Res 14:1167–1174
37. Goulet RW, Goldstein SA, Ciarelli MJ, Kuhn JL, Brown MB, Feldkamp LA (1994) The relationship between the structural and orthogonal compressive properties of trabecular bone. J Biomech 27:375–389

38. Simmons CA, Hipp JA (1997) Method-based differences in the automated analysis of the three- dimensional morphology of trabecular bone. J Bone Miner Res 12:942–947
39. Hildebrand T, Rüegsegger P (1997) A new method for the model independent assessment of thickness in three-dimensional images. J Microsc 185:67–75
40. Goldak JA, Xinhua Y, Knight A, Lingxian D (1991) Constructing discrete medial axis of 3-D objects. Int J Comput Geom Appl 1:327–339
41. Hildebrand T, Rüegsegger P (1997) Quantification of bone microarchitecture with the structure model index. Comput Methods Biomech Biomed Eng 1:15–23
42. Harrigan TP, Mann RW (1984) Characterization of microstructural anisotropy in orthotropic materials using a second rank tensor. J Mater Sci 19:761–767
43. Birkenhager-Frenkel DH, Courpron P, Hupscher EA, Clermonts E, Coutinho MF, Schmitz PI, Meunier PJ (1988) Age-related changes in cancellous bone structure. A two-dimensional study in the transiliac and iliac crest biopsy sites. Bone Miner 4:197–216
44. Eriksen EF, Mosekilde L, Melsen F (1985) Trabecular bone resorption depth decreases with age: differences between normal males and females. Bone 6:141–146
45. Müller R, Hildebrand T, Häuselmann HJ, Rüegsegger P (1996) In vivo reproducibility of three-dimensional structural properties of noninvasive bone biopsies using 3D-pQCT. J Bone Miner Res 11:1745–1750
46. Müller R (2002) The Zurich experience: one decade of three-dimensional high-resolution computed tomography. Top Magn Reson Imaging 13:307–322
47. Van Rietbergen B, Weinans H, Huiskes R, Odgaard A (1995) A new method to determine trabecular bone elastic properties and loading using micromechanical finite-element models. J Biomech 28:69–81
48. Müller R, Rüegsegger P (1995) Three-dimensional finite element modelling of non-invasively assessed trabecular bone structures. Med Eng Phys 17:126–133
49. Boyd SK, Müller R, Zernicke RF (2002) Mechanical and architectural bone adaptation in early stage experimental osteoarthritis. J Bone Miner Res 17:687–694